Lipid-Bound Factor Xa Regulates Tissue Factor Activity†

James Hathcock,* Elena Rusinova, Heikki Vaananen, and Yale Nemerson

Mt. Sinai School of Medicine, Box #1269, Annenberg 24-92, One Gustave Levy Place, New York, New York 10029

Received January 23, 2007; Revised Manuscript Received March 21, 2007

ABSTRACT: The activation of coagulation factor X by tissue factor (TF) and coagulation factor VIIa (VIIa) on a phospholipid surface is thought to be the key step in the initiation of blood coagulation. In this reaction, the product, fXa, is transiently and reversibly bound to the TF−VIIa enzyme complex. This in effect leads to a probabilistic inhibition of subsequent fX activations; a new fX substrate molecule cannot be activated until the old fXa molecule leaves. In this study, we demonstrate that benzamidine and soybean trypsin inhibitor-conjugated Sepharose beads, which bind fXa and sequester it away from the reaction, serve to enhance fX activation by the TF−VIIa complex. Thus, removal of fXa from the reactive zone, by either flow, fXa sequestration, or binding to distant lipid surfaces, can serve to enhance the levels of TF−VIIa activity. Using resonance energy transfer, we found the dissociation constants of fX and fXa for 100 nm diameter phospholipid vesicles to be on the order of 30−60 nM, consistent with previous measurements employing planar lipid surfaces. On the basis of the measurements of binding of fXa to phospholipid surfaces, we demonstrate that the rates of fX activation by the TF−VIIa complex under a variety of experimental conditions depend inversely on the amount of product (fXa) bound to the TF−phospholipid surface. These data support an inhibitory role for the reaction product, fXa, and indicate that models previously employed in understanding this initial coagulation reaction must now be re-evaluated to account for both the product occupancy of the phospholipid surface and the binding of the product to the enzyme. Moreover, the inhibitory properties of fXa can be described on the basis of the estimated surface density of fXa molecules on the TF−phospholipid surface.

In the primary reaction initiating coagulation, TF,[1] which is anchored to a phospholipid surface, forms an enzymatic complex with factor VIIa to activate circulating fX (*1*). This well-studied reaction has typically been described by Michaelis−Menten kinetics where the rate of product formation depends primarily on the delivery of substrate to the enzyme complex and the intrinsic activity of the complex. Although adequate for describing some in vitro experiments, the current models fail to address the complex role of the requisite phospholipid surface and neglect several inconsistent experimental observations, such as a k_{cat} dependence on phospholipid molecules more than 40 nm from the enzyme (*2*). It has previously been shown that the TF−VIIa complex efficiently cleaves fX, which is already bound to the lipid surface (*3*), presumably due to the proper orientation of the scissile bond of fX relative to the lipid-associated gla domain and its strong association with the lipid surface (*2*, *4*). However, the egress of product molecules from the enzyme, their occupancy of the phospholipid surface, and their ability to reversibly bind to the enzymatic complex have not been adequately addressed.

We recently reported (*2*, *5*) evidence indicating the phospholipid surface around the TF−VIIa complex served as a conduit for both the delivery of substrate to the enzyme and the removal of product, which is consistent with the relatively tight binding of both species to the membrane. In the previous study, it was shown that addition of excess lipid vesicles devoid of TF to a reaction mixture containing TF vesicles had dual effects stemming from the fact that lipid vesicles bind both substrate and product. Experiments indicated that if the vesicles contained TF, binding of substrate is clearly acceleratory, whereas binding of product is inhibitory. Conversely, in the absence of TF, binding of substrate is inhibitory and product binding acceleratory. This dual role of phospholipid vesicles introduces ambiguities in defining the reaction mechanisms associated with substrate delivery and product removal. In this study, we resolve some of the issues by demonstrating that STI beads, which specifically bind product without altering the substrate pool, considerably enhance reaction rates, thus enabling us to discriminate the contributions of substrate delivery and product removal.

EXPERIMENTAL PROCEDURES

Materials and Reagents. 1,2-Dioleoyl-*sn*-glycero-3-phosphatidylserine (PS), 1,2-dioleoyl-*sn*-glycero-3-phosphatidylcholine (PC), and 1-palmitoyl-2-hydroxy-*sn*-glycero-3-phosphocholine were purchased from Avanti Polar Lipids (Alabaster, AL). Ultrapure guanidine HCl was from ICN Biomedicals (Aurora, OH). β-Octyl glucopyranoside (βOG) was purchased from Calbiochem (La Jolla, CA). [^{14}C]DOPC,

† Partially supported by NIH Grants P01 HL29019 and P50 HL54469.

* To whom correspondence should be addressed. E-mail: James.Hathcock@mssm.edu. Telephone: (212) 241-7576 or -6083. Fax: (212) 860-7032.

[1] Abbreviations: TF, tissue factor; VIIa, coagulation factor VIIa; fX, coagulation factor X; fXa, coagulation factor Xa; BZA, benzamidine; STI, soybean trypsin inhibitor; RET, resonance energy transfer.

10.1021/bi700136a CCC: $37.00
Published on Web 05/01/2007

N-succinimidyl[2,3-^{3}H] propionate, benzamidine Sepharose 6B, and CNBr-activated Sepharose were from GE Healthcare Life Sciences (Piscataway, NJ). Fluorescent probes Alexa-488 maleimide, Alexa-488 hydroxylamine, and fatty acid BODIPY-558/568 were purchased from Invitrogen (Carlsbad, CA). Silanizing agent F_{13}-OTCS [(tridecafluoro-1,1,2,2-tetrahydrooctyl)trichlorosilane] was from United Chemical Technologies (Bristol, PA). Soybean trypsin inhibitor (STI) was from Sigma (St.Louis, MO) and was conjugated to CNBr-activated Sepharose according to the manufacturer's instructions, yielding 5.58 mg of STI bound per 1 mL of packed resin. Spectrozyme fXa was purchased from American Diagnostica Inc. (Greenwich, CT). Factor VIIa was a gift from Novo Nordisk. Human fX was purified using the method of Miletich (*6*). Human fXa used for activity measurements was prepared by activation of fX with Purified Russel's viper venom; fXa used in phospholipid binding studies was purchased from Enzyme Research Labs (South Bend, IN).

Recombinant human TF_{1-242}, which lacks most of the cytoplasmic domain, was a generous gift from Genentech (San Francisco, CA). Radiolabeled TF, used as a tracer, was tritiated with *N*-succinimidyl[2,3-^{3}H] propionate according to the method described by Bolton and Hunter (*7*), yielding a specific activity of 3.68×10^5 dpm/μg. TF was incorporated into phospholipid vesicles (30/70 PS/PC mixture) as previously described (*2*), and vesicles were extruded to 100 nm diameters by 21 passes through an Avanti Mini Extruder, using a 100 nm pore size membrane. Tracer amounts of [^{3}H]TF and [^{14}C]PC were quantified using a Wallac 1409 counter from Perkin-Elmer (Boston, MA). The TF vesicles used in these studies contained approximately 12 total TF molecules per 100 nm diameter vesicle, six of which are outwardly facing and hence functional (*8*). All lipid vesicles used in this paper were composed of 30% PS and 70% PC and tracer quantities of radiolabels.

Fluorescently labeled fX was prepared via methods similar to those previously described (*9*, *10*). Briefly, the sialic acid residues of fX were oxidized at 4 °C using 2 mM $NaIO_4$ and then coupled to Alexa-488 hydroxylamine (1 h, 20 °C). The resulting bond was stabilized by reduction with 2 mM $NaCNBH_3$ (30 min, 4 °C), yielding approximately 50% labeling of fX. Factor Xa was labeled according to methods described by Bock (*11*, *12*), whereby an Alexa 488-maleimide was coupled via an N^{α}-[(acetylthio)acetyl]-D-Phe-Phe-Arg-CH_2Cl intermediate to the active site of fXa.

Activation of fX by the TF−VIIa Complex. A reaction mixture containing 50 pM total relipidated TF (25 pM exposed TF and 334 nM PSPC), 2 nM fVIIa, and 200 nM fX was prepared in HEPES-buffered saline (HBS) [10 mM HEPES and 140 mM NaCl (pH 7.4)] supplemented with 0.1% bovine serum albumin. All fXa generation assays were performed at 37 °C. The reaction was typically started by the addition of 5 mM $CaCl_2$ and was halted at indicated times by the addition of EDTA (22 mM). For reaction mixtures containing derivatized Sepharose beads, the reaction vials were placed on a rotator for the duration of the reaction before it was quenched with EDTA. FXa was eluted from the BZA and STI-Sepharose with guanidinium chloride (2.3 M, ~30 min), and the beads were removed by rapid centrifugation. Samples (25 μL) of the fXa-containing mixture, either with or without guanidinium, were added to a 96-well plate containing 75 μL of buffer [50 mM EDTA, 50 mM Bicine, and 1 mg/mL BSA (pH 8.5)]. The FXa content was measured by adding 50 μL of a chromogenic substrate (Spectrozyme-Xa, 1.5 mM) and monitoring the rate of change in absorbance at 405 nm. Rates of chromophore generation were compared to fXa standards prepared in identical buffers, either with or without guanidinium. Exposure of fXa standards to 2.3 M guanidinium chloride reduced the amidolytic activity for the chromogenic substrate to 14% of that observed with untreated standards; however, this was more than adequate for detection of the levels of fXa generated in these studies. Changes in the duration of exposure to guanidinium (30−90 min) did not effect the observed activity.

Binding of fXa to BZA and STI-Sepharose. Various concentrations of purified fXa were incubated with a 25% slurry of either BZA or STI-coupled Sepharose beads for 30 min. The beads were removed by centrifugation (60 s at 16000*g*), and the supernatant concentration of fXa was determined as described above. In some studies, the bound fXa was eluted from the beads with guanidium and the amount measured as described above.

Binding of fX and fXa to Phospholipid Vesicles. The binding of fX to vesicles was assessed by resonance energy transfer (RET) between an Alexa-488 probe attached to the sialic acid residues of fX and a BODIPY-conjugated PC incorporated into the lipid vesicle. Using an SLM Aminco 500C spectrofluorometer (450 nm excitation), the fluorescence emission (518 nm) of the labeled protein was measured as 100 nm diameter phospholipid vesicles containing 1 mol % BODIPY-PC were titrated into a silanized cuvette, all at 37 °C. As fX, or fXa, bound to the lipid surfaces, the observed fluorescence was quenched due to the transfer of energy between the Alexa donor and the BODIPY acceptor. The energy transfer was defined as $1 - F/F_o$, where F is the observed fluorescence and F_o is the fluorescence observed in the absence of acceptor. To determine the dissociation constant (K_D), a Levenberg−Marquardt algorithm was used to fit the magnitude of energy transfer to a function of the total lipid added, where L is the lipid concentration, XPL is the stoichiometry of lipid to fX molecules, and fXa is the concentration of fXa. As the measured signal indicates relative and not absolute binding of protein to lipid, we employ previously published XPL values in fitting the function to our data (*2*).

$$\text{signal} = \frac{(-b - \sqrt{b^2 - 4c})}{2} \frac{(\text{max signal})}{\text{fXa}}$$

$$b = L/\text{XPL} + K_d + \text{fXa}$$

$$c = (\text{fXa} \cdot L)/\text{XPL}$$

Estimation of Reaction Velocities and fXa Surface Densities. To determine the key parameters regulating fXa formation in full time course experiments, the instantaneous reaction velocities as well as the relative lipid surface densities of fX and fXa were estimated for each experimental time point. Instantaneous reaction velocities were estimated from the product concentration measurements as the quotient of the change in product concentration between sample intervals and the duration of the sampling interval, employing

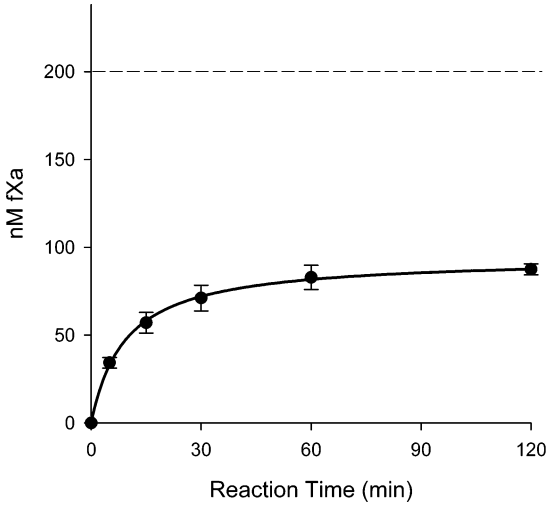

FIGURE 1: Full time course of activation of fX (200 nM) by the TF−VIIa complex. After 120 min of reaction time, the TF−VIIa complex activity ceased after converting less than half of the "available" substrate molecules. Traditional Michaelis−Menten treatments dictate the reaction should proceed as long as substrate remains.

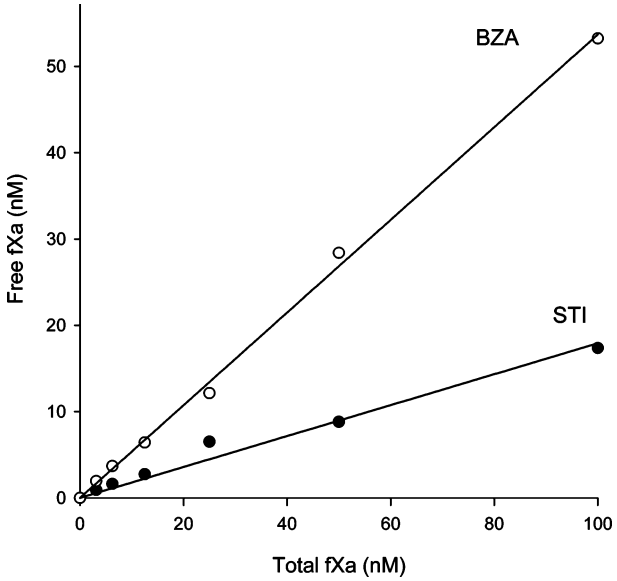

FIGURE 2: Binding of fXa to BZA- and STI-coated Sepharose beads. In the presence of a 25% BZA−Sepharose slurry (○), approximately half of the total fXa molecules (in the experimental range of 0−100 nM fXa) were localized to the Sepharose beads. STI-coated Sepharose beads (●) were stronger, binding approximately 80% of the fXa molecules.

a backward difference method (*13*). Thus, for each experimental time point, the reaction velocity, the total product concentration, and the remaining substrate concentration were known. In addition, on the basis of the experimentally determined binding relationships between fXa and STI beads, it was possible to estimate the fraction of fXa not bound to STI beads. To determine the amount of fX and fXa bound to the surfaces of the lipid vesicles, we simulated the competition of fX and fXa (not bound to STI beads) as described previously (*2*). Briefly, a series of coupled, first-order differential equations describing the binding of fX and fXa to phospholipid was solved in FORTRAN using the Livermore Labs ordinary differential equations solver (LSODE). The lipid binding capacities used in these simulations were based on ellipsometry (*4*) and lipid dissociation constants measured via RET.

RESULTS

Full Time Course of fX Activation by the TF−VIIa Complex. To examine the full time course of activation of fX by the TF−VIIa complex, 5 mM $CaCl_2$ was added to a reaction mixture containing 200 nM fX, 2 nM fVIIa, and TF vesicles (25 pM exposed TF, 334 nM PSPC, 100 nm diameter vesicles, approximately six exposed TF molecules per vesicle), and the resulting levels of fXa were assayed at specified intervals. Factor Xa formation was rapid over the first 15 min of the reaction, but had almost ceased by 60 min (Figure 1); the fXa concentration increased by less than 5% over the second hour. Interestingly, the reaction ceased even though the remaining fX concentration was 113 nM, far above the reported K_M for such TF vesicles (*2*). Classical Michaelis−Menten treatments of this reaction dictate the reaction should proceed as long as the substrate remains available. As the substrate concentration did not appear to be limiting, we investigated product-inhibition effects on the reaction.

Binding of fXa to BZA and STI-Conjugated Sepharose. To test the hypothesis that product molecules downregulated TF−VIIa activity, we sought reagents that would specifically bind and sequester fXa, thereby minimizing product inhibition effects without disturbing the available substrate pool. Accordingly, we investigated the binding of fXa to BZA and STI-conjugated resins. Experimentally, we found BZA-coupled Sepharose beads (25%, v/v) bound approximately 44% of the total fXa in a mixture containing less than 100 nM fXa (Figure 2). Briefly, a known concentration of fXa was incubated for 15 min on a rocker with BZA-Sepharose beads. The beads were then centrifuged, and the supernatant fXa concentration was assayed. Similar studies with STI-coated Sepharose indicated it was a much stronger binder, sequestering approximately 83% of the total fXa (0−100 nM).

Product Removal Enhances TF−VIIa Complex Activity. To investigate the effects of the reaction product, fXa, on TF−VIIa activity, we monitored the full time course of TF−VIIa-mediated fX activation in the presence of BZA or STI-conjugated Sepharose beads. These reagents specifically bound fXa, segregating endogenously generated fXa from the TF vesicles and thereby minimizing the interactions of the product with TF−fVIIa on vesicle surfaces. Due to relative collisional frequencies, we expect the STI-Sepharose beads primarily bound and sequestered solution-phase fXa while having little direct effect on fXa already bound to vesicle surfaces. A reaction mixture containing 200 nM fX, 2 nM fVIIa, TF vesicles (25 pM exposed TF, 334 nM PSPC, 100 nm diameter vesicles), and derivatized sepharose beads was initiated by the addition of 5 mM $CaCl_2$. At indicated intervals, the reaction was stopped with EDTA (22 mM). To quantify the total fXa generated, guanidinium chloride (2.3 M) was added to dissociate fXa from the BZA- or STI-coupled beads, and the beads were removed by centrifugation. The fXa concentration was then quantified using a chromogenic assay.

In the presence of BZA-Sepharose (25%, v/v), the rate of fX activation was substantially faster than that observed with controls (inert Sepharose beads or mock buffer in lieu of

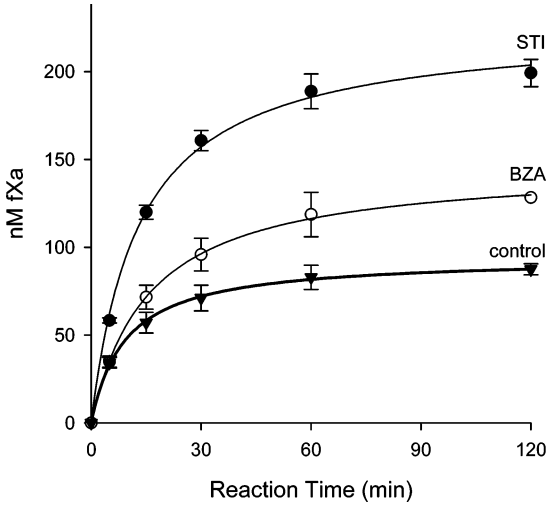

FIGURE 3: Sequestering of fXa accelerates fX activation. The addition of BZA-coated beads (○) to a reaction mixture containing the TF−VIIa complex and fX (200 nM, initial) served to bind fXa away from the TF−VIIa vesicles, thereby accelerating TF−VIIa activity and allowing higher levels of substrate conversion. Addition of the stronger-binding, STI-coated beads (●) greatly enhanced the rate of fX activation and allowed virtually all of the substrate molecules to become activated.

beads), and the levels of fXa found at 60 min were approximately 44% higher than controls (Figure 3). Thus, BZA beads enhanced the rates of fX activation presumably by segregating the reaction product, fXa, from the TF vesicles. Additional experiments with varying amounts of BZA beads (0−25% slurry) indicated the increase in the level of product formation was dependent on the quantity of BZA beads (data not shown). Similar experiments with STI beads, a stronger fXa binder, revealed a more marked increase in the rates of fX activation and, by 2 h, had resulted in the complete activation of all available substrate. Thus, the observed reaction rates and degree of substrate consumption depended strongly on product removal (Figure 3).

In control studies, STI beads were added to the reaction mixture 60 min after the onset of the reaction to verify that the TF−VIIa complex remained functional and that the substrate remained available. Although the reaction rates had slowed to nearly zero by 60 min, the addition of STI beads resulted in the rapid resumption of fX activation, indicating that fully functional fX and fVIIa remained present in the reaction mixture. Hence, the observed inhibition could be attributed to product inhibition effects of fXa, and not degradation of fX or fVIIa.

Binding of fX and fXa to PSPC Surfaces. As the activation of fX takes place on a phospholipid surface, in this case 100 nm diameter vesicles, the relationship between free fXa molecules and those bound to the TF−phospholipid surface is of particular interest. The binding of fX to vesicles was assessed by resonance energy transfer (RET) between Alexa-488 conjugated to the sialic acid residues of fX, chosen because the carbohydrates have not been implicated in binding, per se, and a BODIPY-conjugated PC incorporated into the lipid vesicles (1 mol %). Extruded vesicles containing the BODIPY acceptor were sequentially added to a silanized cuvette containing 100 nM labeled fX (5 mM $CaCl_2$, 0.2 mg/mL ovalbumin, HBS), and the decrease in fluorescence at 488 nm due to binding was monitored. Figure 4 shows the transfer efficiency associated with fX binding to lipid as a function of the total lipid added. The equations for bound fX as a function of total lipid and total fX (see Experimental Procedures) were fit to the experimental data sets ($n = 3$) to determine the dissociation constant.

Assuming 106 phospholipid molecules are associated with each molecule of bound fX (*2*), a Levenberg−Marquardt fit indicated a K_D of 61 ± 9 nM for fX binding. The dissociation constant of fXa was measured in a similar fashion using active site-labeled (Alexa488) fXa. We have previously shown that at saturation twice as many molecules of fXa are bound compared to fX (*2*). Assuming 53 phospholipid molecules per bound fXa (*2*), a K_D of 31 ± 4.6 nM was calculated. These binding constants, observed with curved 100 nm diameter vesicles, are similar to previously reported values for binding of fX and fXa to planar acidic phospholipid surfaces (*4*) and allowed us to estimate the competitive binding of fX and fXa to vesicle surfaces.

Lipid-Bound fXa Regulates fX Activation. The experiments with BZA and STI beads described above demonstrate that product removal enhances TF−VIIa-mediated fX activation. However, the mechanism by which fXa impedes TF−VIIa activity and the key parameters that regulate fX activation remain unclear. To this end, the instantaneous rates of fXa generation were estimated for each data point shown in Figure 3 using a backward difference scheme and plotted as a function of the respective substrate concentration (Figure 5a). Although the reaction rates correlated with substrate concentration as expected, experimental data points with equivalent substrate concentrations had vastly different reaction rates. Similarly, reaction rates anticorrelated with total product concentrations, but this parameter did not reconcile differences in the observed reaction rates with and without STI beads (Figure 5b). Using the relationships derived from Figure 2, we also show the reaction rates as a function of the fXa not bound to STI beads (Figure 5c). As this fraction of fXa competes for access to the TF vesicle, we hypothesized it would be a key parameter regulating the observed reaction rates. Interestingly, this parameter also failed to reconcile differences in the reaction rates observed with and without STI beads.

On the basis of binding measurements of fX and fXa to acidic phospholipid surfaces (*2*), we simulated the competitive binding of fX and fXa molecules for the vesicle surface on which TF resides. These numerical simulations, which have been described previously (*2*), are based on equilibrium conditions and thereby serve only to estimate the fraction of the lipid surface occupied by fX or fXa. When the reaction rates are plotted as a function of the percentage of the TF−vesicle surface occupied by fXa (Figure 5d), both data sets coincide indicating that lipid-bound fXa is the key parameter regulating the observed reaction rates.

DISCUSSION

Whereas most studies of TF−VIIa activity focus on the "initial rate" of fX activation, few published reports have thus far addressed the full time course of fX activation by the TF−VIIa complex. One early study (*14*), using fVIIa to regulate the number of functional TF−VIIa complexes, showed that the rate of fX activation slowed to zero well before all of the substrate was consumed. The authors

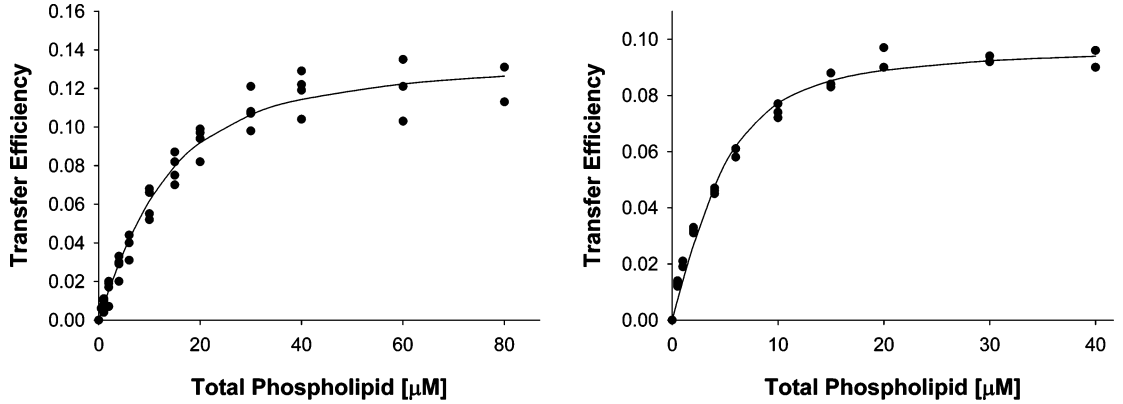

FIGURE 4: Binding of fX (left) and fXa (right) to 100 nm diameter phospholipid vesicles (30/70 PS/PC) by RET. Transfer efficiency (ordinate) indicates relative binding of donor-labeled protein to acceptor-labeled lipid.

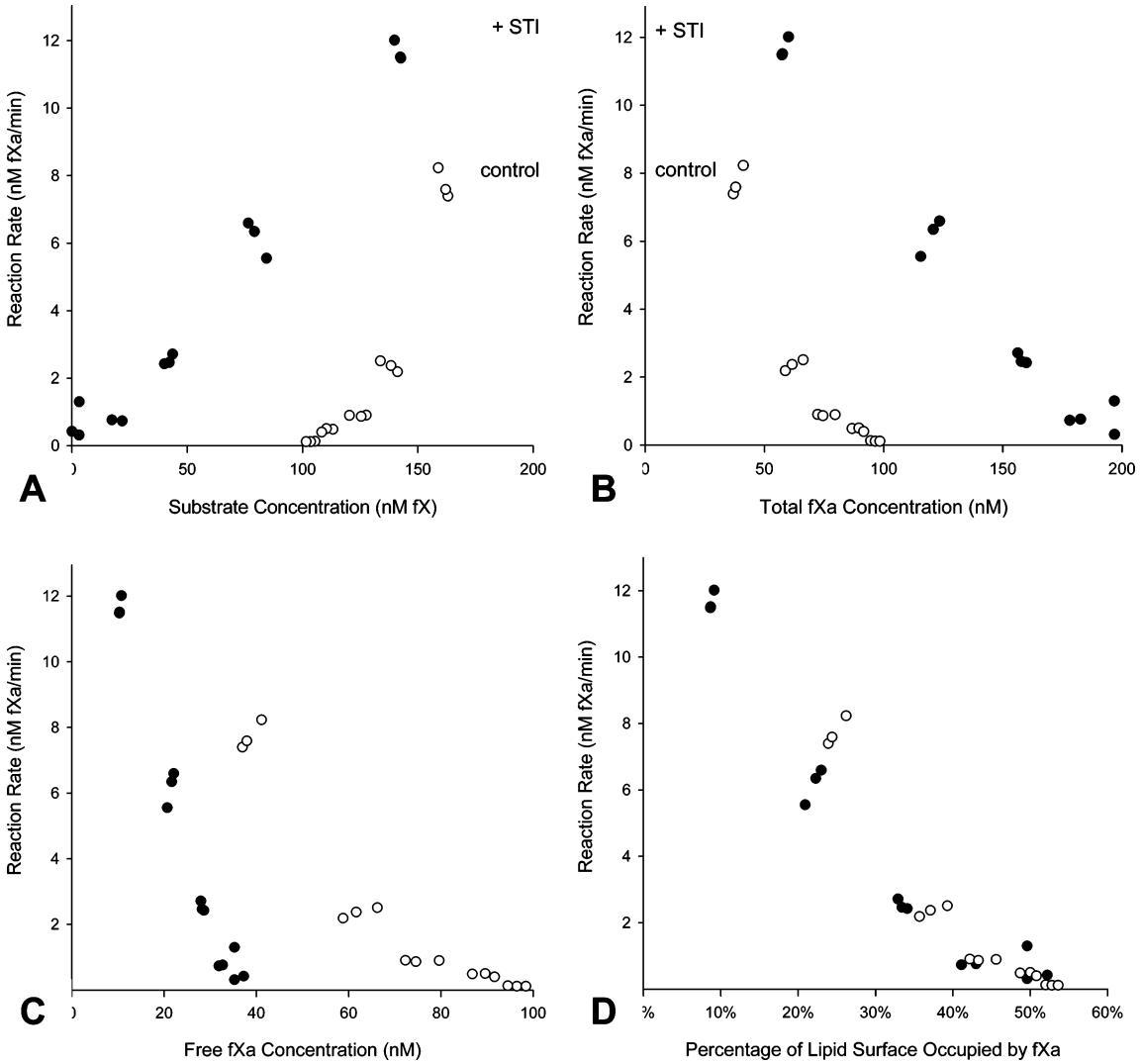

FIGURE 5: Lipid-bound fXa regulates TF−VIIa complex activity. Although the instantaneous reaction velocities from studies with (●) or without (○) STI beads are (A) correlated with the total substrate concentration and (B) anticorrelated with the total fXa concentration, these parameters do not reconcile the different velocities observed in the presence or absence of the STI-coated beads. (C) Interestingly, the free fXa concentration (not bound to Sepharose) also fails to reconcile the different velocities observed with and without beads. (D) However, simulations of binding of fX and fXa to vesicles do indicate that all the experimental reaction velocities are regulated by the percentage of the lipid surface area occupied by fXa.

reasoned that inactivation of fVIIa by fXa greatly reduced the number of functional enzyme complexes, thereby preventing the reaction from reaching completion. A much later study by a different group found a markedly different result, namely that all of the fX was completely converted to fXa within a matter of minutes (*3*). In our study, we found that in the presence of limiting concentrations of TF vesicles and an excess of fVIIa, the reaction rate eventually slows to zero with less than half of the available substrate being converted. Moreover, we demonstrated that in our reaction mixtures,

functional fVIIa was present after the reaction had ceased.

As recent reports by our group (*2*, *5*) and others (*15*) have indicated that the reaction product, fXa, can inhibit TF−VIIa complex activity, we extended our findings to determine whether product inhibition effects were responsible for terminating the reaction and thereby limiting substrate consumption. When the activation of fX was performed in the presence of STI beads capable of sequestering fXa, the reaction velocities were dramatically enhanced, even during the first 5 min of the reaction, and the levels of substrate activation increased from 83 to 200 nM, i.e., complete activation. Thus, the TF−VIIa reaction is self-damping with product inhibition effects overtly evident during the initial minutes of the reaction. Hence, all initial rate-type measurements designed to infer the kinetics of the TF−VIIa complex must be influenced by product inhibition effects.

In this study, we observed that reactions occurring under identical starting substrate concentrations proceeded at vastly different rates depending on the presence of STI beads (Figure 5a). Though the purpose of the STI beads was to sequester solution-phase fXa, thereby minimizing product inhibition effects, a plot of the experimental reactions rates versus the solution-phase concentrations of fXa did not reconcile differences in the reaction rates with and without STI (Figure 5c).

As substrate−enzyme interactions and likely product−enzyme interactions occur on the lipid surface, we performed lipid binding studies to estimate the surface densities of fX and fXa. Although numerous measurements are reported in the literature for binding of fX and fXa to acidic phospholipids, the reported values for the dissociation constants vary by several orders of magnitude (*2*). Energy transfer studies indicated the dissociation constants for binding of fX and fXa to acidic phospholipid vesicles were on the order of 60 and 30 nM, respectively, which are similar to other published values using light scattering (*16*), surface plasmon resonance (*4*), and ellipsometric (*2*) techniques. In addition, there do not appear to be substantial differences in the binding of fX and fXa to the surfaces of 100 nm diameter curved vesicles as compared to previous reports using planar phospholipid bilayers (*2*, *4*, *17*).

With confidence in the vesicle binding properties of fX and fXa, we estimated the lipid surface densities of fX and fXa for each experimental fXa measurement shown in Figure 3. Interestingly, all the instantaneous reaction velocity data appeared to be anticorrelated with the estimated surface densities of fXa, regardless of whether STI beads were present. Hence, the local surface density of fXa on the TF−vesicle surface appears to be a key regulator of TF−VIIa activity (Figure 5d).

In a recently published study, we hypothesized that the presence of lipid vesicles devoid of TF could have dual effects on TF−VIIa activity, either diminishing TF−VIIa activity by binding fX and lowering the effective substrate concentration or accelerating the reaction by virtue of binding the inhibitory product. These findings using STI beads, which specifically bind fXa without affecting the substrate, have helped confirm this hypothesis by demonstrating that fXa removal does indeed accelerate TF−VIIa-mediated fXa activation.

Given these findings, we were puzzled about how a previous study using a single progress curve fit to an integrated form of the Michaelis−Menten equation reported complete activation of fX within minutes of starting the reaction. Upon further inspection, we found these investigators used, without comment, extraordinarily high concentrations of phospholipid (~600 μM). In fact, although their vesicles were not extruded to uniform dimensions, had they been ~100 nm structures, these investigators would have had 9.3 vesicles for every functional enzyme complex. Our current data suggest that this very high lipid concentration served as a fXa trap thereby allowing the reaction to achieve completion. In addition, the excess lipid likely acted as a sink for fX, as reflected by the very high K_M (1.5 μM vs ~15 nM for the TF preparations used in this paper).

Although these experiments demonstrate that removal of solution-phase fXa accelerates fX activation, the fXa generated by the TF−VIIa complex does not originate in solution but rather on the lipid surface directly adjacent to the TF−VIIa complex. Because solution-phase fX and fXa compete for lipid binding sites and hence access to the enzyme, the product inhibition effects resulting from binding of solution-phase fXa "back" to the surface of the TF vesicle are likely manifested as an increase in the apparent K_M of the reaction. Hence, the STI beads primarily serve to relieve competitive product inhibition effects. Thus, physiologic lipid surfaces that bind fXa away from the TF−VIIa complex or flow conditions that transport fXa downstream may serve to competitively enhance rates of TF−VIIa-mediated fXa formation. In contrast, newly generated fXa molecules are not spatially equivalent to those in solution or to other fXa molecules a finite distance from the TF−VIIa complex on the vesicle surface, and thus, the inhibition is more complex.

The primary mechanism by which lipid-bound fXa inhibits its own formation remains unclear, as multiple pathways of inhibition exist. As fXa is *ipso facto* bound to the TF−VIIa complex during the activation process and structural studies have identified exosite interaction regions between fXa and the TF−VIIa complex (*18*, *19*), fXa likely binds reversibly to the enzyme complex. In addition, lipid-bound fXa occupies the conduit through which substrate reaches enzyme and thus prevents binding of substrate to surface as well as the lateral diffusion of bound substrate toward the enzyme. Also, in the presence of limited quantities of fVIIa, fXa may inhibit the reaction by proteolyzing fVIIa (*20*); however, this mechanism is likely slow as numerous fXa molecules can be generated at the site of the enzyme without a loss of function. As a result of these complex inhibition pathways, classic competitive inhibition constants, i.e., K_i, are unlikely to be meaningful in systems with varying quantities of lipid, or different spatial arrangements of TF and phospholipid. In fact, we have previously shown the inhibitory potency of exogenously added fXa varies according to the quantity of lipid associated with each TF−VIIa complex (*2*). These complex effects underlie our recently introduced concept of an "active" phospholipid radius required for efficient catalysis (*2*, *5*). Two-dimensional stochastic modeling of fX activation on surfaces should greatly aid in our understanding of how these molecules move and interact on a lipid surface.

REFERENCES

1. Hathcock, J. (2004) Vascular biology: The role of tissue factor, *Semin. Hematol. 41*, 30−34.
2. Hathcock, J. J., Rusinova, E., Gentry, R. D., Andree, H., and Nemerson, Y. (2005) Phospholipid regulates the activation of factor X by tissue factor/factor VIIa (TF/VIIa) via substrate and product interactions, *Biochemistry 44*, 8187−8197.
3. Krishnaswamy, S., Field, K. A., Edgington, T. S., Morrissey, J. H., and Mann, K. G. (1992) Role of the membrane surface in the activation of human coagulation factor X, *J. Biol. Chem. 267*, 26110−26120.
4. Erb, E. M., Stenflo, J., and Drakenberg, T. (2002) Interaction of bovine coagulation factor X and its glutamic-acid-containing fragments with phospholipid membranes. A surface plasmon resonance study, *Eur. J. Biochem. 269*, 3041−3046.
5. Hathcock, J. J., Rusinova, E., Andree, H., and Nemerson, Y. (2006) Phospholipid surfaces regulate the delivery of substrate to tissue factor:VIIa and the removal of product, *Blood Cells, Mol., Dis. 36*, 194−198.
6. Miletich, J. P., Broze, G. J., and Majerus, P. W. (1981) Purification of human coagulation factors II, IX and X using sulfated dextran beads, *Methods Enzymol. 80*, 221−228.
7. Bolton, A. E., and Hunter, W. M. (1973) The labelling of proteins to high specific radioactivities by conjugation to a ^{125}I-containing acylating agent, *Biochem. J. 133*, 529−539.
8. Bach, R., and Gentry, R. Y. N. (1986) Factor VII binding to tissue factor in reconstituted phospholipid vesicles: Induction of cooperativity by phosphatidylserine, *Biochemistry 25*, 4007−4020.
9. Silverberg, S. A., Nemerson, Y., and Zur, M. (1977) Kinetics of the activation of bovine coagulation factor X by components of the extrinsic pathway. Kinetic behavior of two-chain factor VII in the presence and absence of tissue factor, *J. Biol. Chem. 252*, 8481−8488.
10. Morrison, S. A., and Jesty, J. (1984) Tissue factor-dependent activation of tritium-labeled factor IX and factor X in human plasma, *Blood 63*, 1338−1347.
11. Bock, P. E. (1992) Active-site-selective labeling of blood coagulation proteinases with fluorescence probes by the use of thioester peptide chloromethyl ketones. II. Properties of thrombin derivatives as reporters of prothrombin fragment 2 binding and specificity of the labeling approach for other proteinases, *J. Biol. Chem. 267*, 14974−14981.
12. Bock, P. E. (1993) Thioester peptide chloromethyl ketones: Reagents for active site-selective labeling of serine proteinases with spectroscopic probes, *Methods Enzymol. 222*, 478−503.
13. Hamming, R. (1987) *Numerical Methods for Scientists and Engineers*, Dover Publications, Mineola, NY, p 162.
14. Nemerson, Y., Silverberg, S. A., and Jesty, J. (1974) Self-Damping Mechanism in Blood Coagulation, *Thromb. Diath. Haemorrh. 32*, 57−63.
15. Lu, G., Broze, G. J., Jr., and Krishnaswamy, S. (2004) Formation of factors IXa and Xa by the extrinsic pathway: Differential regulation by tissue factor pathway inhibitor and antithrombin III, *J. Biol. Chem. 279*, 17241−17249.
16. McDonald, J. F., Shah, A. M., Schwalbe, R. A., Kisiel, W., Dahlback, B., and Nelsestuen, G. L. (1997) Comparison of naturally occurring vitamin K-dependent proteins: Correlation of amino acid sequences and membrane binding properties suggests a membrane contact site, *Biochemistry 36*, 5120−5127.
17. Andree, H. A. M., Contino, P. B., Repke, D., Gentry, R., and Nemerson, Y. (1994) Transport rate limited catalysis on macroscopic surfaces: The activation of factor X in a continuous flow enzyme reactor, *Biochemistry 33*, 4368−4374.
18. Norledge, B. V., Petrovan, R. J., Ruf, W., and Olson, A. J. (2003) The tissue factor/factor VIIa/factor Xa complex: A model built by docking and site-directed mutagenesis, *Proteins 53*, 640−648.
19. Kirchhofer, D., Eigenbrot, C., Lipari, M. T., Moran, P., Peek, M., and Kelley, R. F. (2001) The tissue factor region that interacts with factor Xa in the activation of factor VII, *Biochemistry 40*, 675−682.
20. Radcliffe, R., and Nemerson, Y. (1975) Activation and control of factor VII by activated factor X and thrombin. Isolation and characterization of a single chain form of factor VII, *J. Biol. Chem. 250*, 388−395.

BI700136A